Available online at www.sciencedirect.com

ELSEVIER

Journal of Volcanology and Geothermal Research 136 (2004) 141–158

Journal of volcanology and geothermal research

www.elsevier.com/locate/jvolgeores

Distribution and characteristics in waveform and spectrum of seismic events associated with the 2000 eruption of Mt. Usu

Wakana Matsubara[a,1], Kiyoshi Yomogida[a,*], Junji Koyama[a], Minoru Kasahara[b], Makoto Ichiyanagi[b], Hitoshi Kawakatsu[c], Mare Yamamoto[c]

[a] *Division of Earth and Planetary Sciences, Graduate School of Science, Hokkaido University, Sapporo 060-0810, Japan*
[b] *Institute of Seismology and Volcanology, Graduate School of Science, Hokkaido University, Sapporo 060-0810, Japan*
[c] *Earthquake Research Institute, University of Tokyo, 1-1-1 Yayoi, Bunkyo-ku, Tokyo 113-0032, Japan*

Abstract

We installed five broadband seismometers around Mt. Usu, Hokkaido, Japan, just before the first surface eruption on March 31, 2000. By using these broadband data with short-period seismograms recorded by Japan Meteorological Agency and Institute of Seismology and Volcanology of Hokkaido University, we located 590 earthquakes associated with the 2000 eruption of Mt. Usu from March 31, 12:58 to April 5, 2000, including 41 low-frequency earthquakes. Low-frequency earthquakes have clear predominant frequencies of about 1.0–1.5 Hz. While the seismicity of tectonic earthquakes was still active on April 5, there were almost no low-frequency events after April 2. All the low-frequency earthquakes occurred within a vertical and narrow zone near the craters of eruption, and they are shallower than 4 km. In contrast, the active area of tectonic earthquakes spreads out in a large area, particularly deep in the south of the craters. From these temporal and spatial patterns, together with GPS and gravity measurements that support the termination of magma activities before April 2, we suggest that low-frequency earthquakes were caused by magma or hydrothermal activities beneath the volcano while tectonic ones were caused by the regional tectonic stress affected by the intrusion of magma body near the craters. Related to long-term magma activities of this eruption, four deep crustal low-frequency events were identified on October 17, 1998 just in the south of Mt. Usu in the depth range of 20–30 km. As proposed for other active volcanoes, these deep crustal events may represent a part of deep magma activities beneath Mt. Usu.

Keywords: low-frequency earthquake; Usu volcano; volcanic eruption; hypocentral distribution; deep crustal earthquake

1. Introduction

In the 20th century, Mt. Usu located in southwestern Hokkaido, Japan, erupted four times: in 1910, 1943, 1977 and 2000. Each eruption was accompanied by persistent seismic activity and remarkable crustal deformation, including the formation of lava domes or cryptodomes. These volcanic eruptions are characterized by dacitic magma of high viscosity. The difference among the four volcanic activities should depend on the state of the volcano at each eruption, including physical conditions of magma and vent structures of eruption sites, as well as the presence of aquifer (Okada et al., 1981; Yokoyama and Seino, 2000).

* Corresponding author. Tel.: +81-11-706-2758; fax: +81-11-746-2715.
E-mail address: yomo@ep.sci.hokudai.ac.jp (K. Yomogida).
[1] Present address: Asia Air Survey Co., LTD., 1-2-2, Manfuku-ji, Asabu-ku, Kawasaki 215-0004, Japan.

0377-0273/$ - see front matter © 2004 Elsevier B.V. All rights reserved.
doi:10.1016/j.jvolgeores.2004.05.016

Volcanic earthquakes and tremors have quite different characters from earthquakes caused by fault motion due to ambient tectonic stress (hereafter called "tectonic earthquakes"). Many previous studies showed that they are caused by underground magma or hydrothermal activities. Although the style of volcanism, either liquid-like basaltic magma such as Kilauea (e.g., Aki and Koyanagi, 1981; Ohminato et al., 1998) or dacitic magma such as Mt. Rebout (e.g., Chouet et al., 1994), shows very different values of the involved parameters, their overall source process appears to be explained in a rather unified manner (Chouet, 1996). In order to understand the dynamics beneath active volcanoes, broadband seismograms seem to contain a lot of information in a wide frequency range. Broadband seismic observations at volcanic areas have revealed many new phenomena related to magma or hydrothermal activities beneath volcanoes: for examples, Sakurajima volcano in Japan by Kawakatsu et al. (1992) and Tsuruga et al. (1997), and Mt. Aso by Kaneshima et al. (1996) and Kawakatsu et al. (2000).

It is known that there were little seismicity and/or long-term precursory phenomena in general that preceded each eruption of Mt. Usu, except for nearly six-month activities before the 1944 main eruption (e.g., Yokoyama and Seino, 2000). The seismic activity related to the 2000 eruption also became intensified suddenly on March 27, 2000. This unique characteristic of Mt. Usu made it possible to release the official warning announcement to its local residents, and they could be evacuated before the first surface eruption on March 31 from its northwestern flank (see Figs. 1 and 2). Just before the first visible eruption, we installed five broadband seismometers around the mountain and kept the observation by November 4, 2000. Using these seismograms recorded continuously, we found long-period tremors whose predominant period is about 12 s, recorded for the first week after the eruption (Yamamoto et al., 2002).

In this paper, we located 590 earthquakes associated with the 2000 eruption of Mt. Usu in the period from March 31 12:58 to April 5, followed by some waveform analyses. In addition, low-frequency earthquakes in the lower crust (20–30 km deep) occurred near Mt.Usu in 1998, and we discuss the relationship between these deep crustal low-frequency events and the 2000 eruption of Mt. Usu.

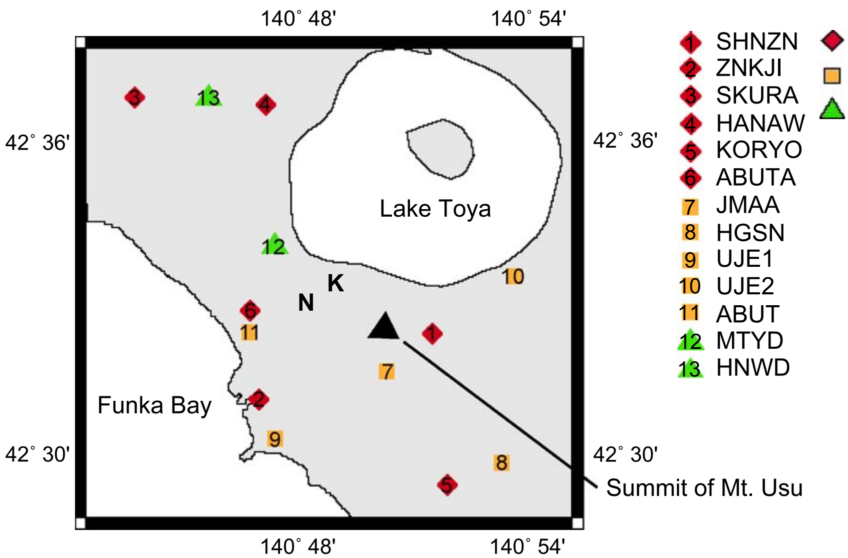

Fig. 1. Location map of broadband seismic stations (in red), JMA short-period seismic stations (in orange), ISV short-period seismic stations (in green). The two letters, "*N*" and "*K*", indicate the locations of the craters created by the 2000 eruption of Mt. Usu ("N": Nishiyama craters, "K": Kompira craters).

2. Data

Seismicity around Mt. Usu was low for a long time. Hypocentral locations determined by the routine work of Institute of Seismology and Volcanology (ISV, Hokkaido University) show that there was no anomalous seismicity around Mt. Usu for several days before the 2000 eruption. The seismicity became active only from March 27, 2000. Strong-motion seismometers and GPS instruments had been temporally installed around the mountain before the eruption on March 31. We installed five broadband seismometers (Gerulp CMG-3T seismometer + HAKUSAN LS8000WD recorder) surrounding the mountain. The first station (SHNZN) was installed at 12:58 on March 31, 2000 (hereafter, we shall use the corresponding local time system, Japan Standard Time), just before the first eruption. The other stations were installed after the first eruption, surrounding craters that were created by series of subsequent eruptions. Although we had continued the observation using broadband seismometers for about 7 months, the seismicity virtually diminished within 1 month after the first eruption. In this study, we analyzed seismic events for the first 6 days of our observation period, from March 31 to April 5, 2000, when the number of daily seismic events was very high.

We use data collected by our seismic network composed of the above mentioned five three-component broadband stations (six station locations in total), together with data of three-component 1 Hz seismometers by five JMA (Japan Meteorological Agent) and two ISV stations. The sampling rate of all seismometers is 100 Hz. The locations of these stations are

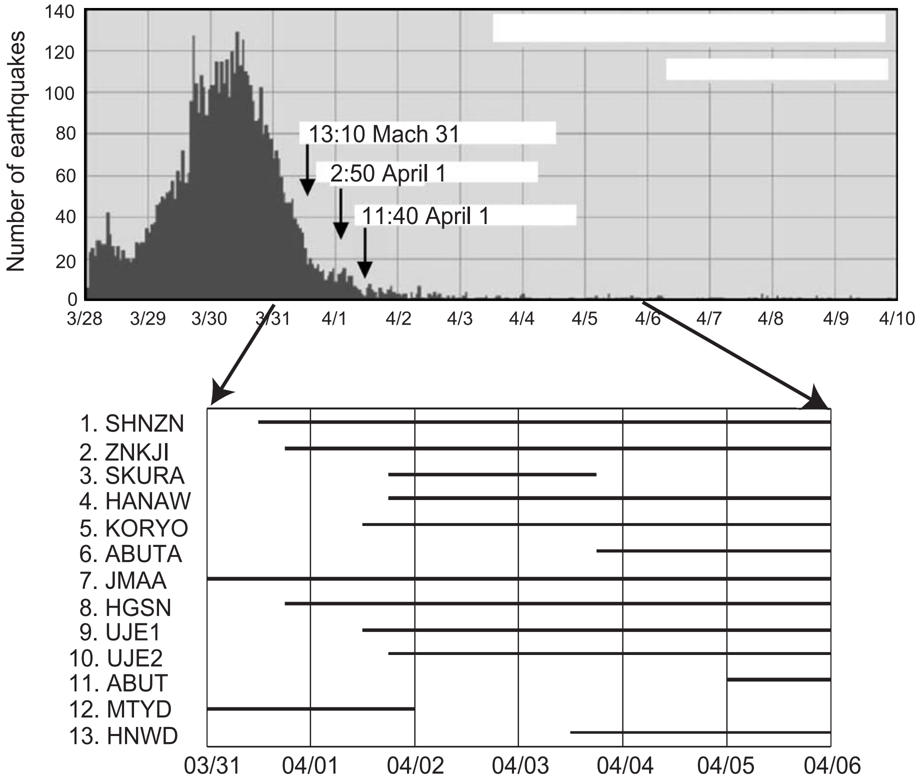

Fig. 2. Observation period of each seismic station with the overall temporal variation of earthquakes associated with the 2000 Mt. Usu eruption. The number of earthquakes is defined by the events whose maximum amplitude of seismograms recorded at Muroran Branch of Japan Meteorological Agency was larger than 3 μm. The remarked timings correspond to (1) the first surface eruption at Nishiyama craters at 13:10 on March 31, (2) another large eruption at 2:50 on April 1 and (3) the first eruption at Kompira craters at 11:40 on April 1. The numbers assigned to station codes correspond to those in Fig. 1 (modified from Geological Survey of Hokkaido, 2000).

shown in Fig. 1, and the operation period of each station in Fig. 2 with the seismicity during the eruption period (Geological Survey of Hokkaido, 2000), using the code "SAC2000" (Goldstein et al., 1999). Although the seismic activity was the highest on the first day (March 31, 2000), the station coverage was poor. It was gradually improved as the time passed by.

3. Hypocenter determination

We used the code named 'HYPOMH' (Hirata and Matsu'ura, 1987) to determine hypocenters. We picked arrival times of P and S waves with the "WIN" system (Urabe and Tsukada, 1991), and located 590 events where P-wave and/or S-wave onsets can be clearly identified at more than four stations. We determined event locations both with and without station corrections, but any systematic discrepancies were observed between the two results, probably because none of stations were located on very thick volcanic materials solidified not well. Although we tested several different velocity models with variations in velocity up to 10% in order to check the effect of the uncertainty in velocity model on hypocenter locations, they showed no significant changes for events not shallower than 2 km. This is partly because stations were distributed around the hypocentral area relatively uniformly with the interval of about 2 km, as shown in Fig. 1. We adopted a velocity model with one surface layer changing linearly from $V_p = 3.0$ km/s to $V_p = 5.0$ km/s within 10 km, and the next layer changing linearly from $V_p = 5.0$ km to $V_p = 8.0$ km/s within 100 km, following the model of ISV for the routine hypocenter determination in this area. The V_p/V_s ratio is assumed to be $\sqrt{3}$ at every depth.

As mentioned in the Introduction, some recorded seismograms clearly indicate the occurrence of so-

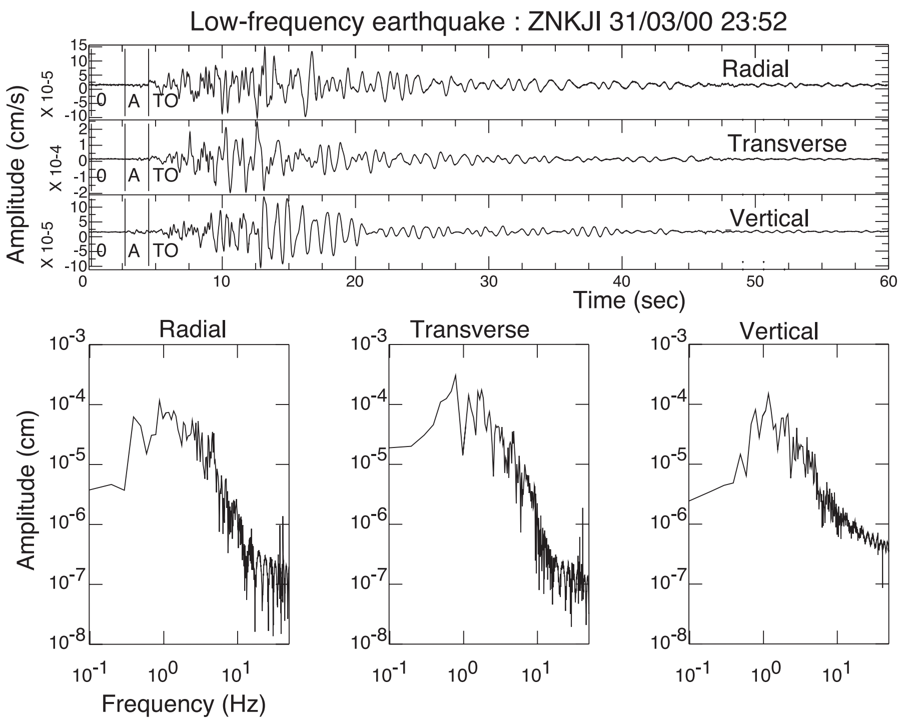

Fig. 3. Example of seismograms and S-wave spectra of a low-frequency earthquake, observed at a broadband seismic station, ZNKJI. Letters "O", "A" and "TO" in seismograms represent the estimated origin time, the picked onset time and the predicted arrival time of S wave, respectively.

called "low-frequency earthquakes" that are commonly observed in active volcanoes. We classified recorded events into two types: (1) low-frequency earthquakes with the predominant frequency of about 1 Hz, and (2) tectonic earthquakes with a clear onset of P-wave arrival and predominant frequencies higher than several Hz, as shown in Figs. 3 and 4, respectively. Amplitude spectra of S wave are shown in the lower part of each figure. S-wave spectra were calculated with the time window of 10 s from the S-wave onset although some energy of surface waves may be contaminated in the tectonic earthquake case.

During the period from March 31 to April 5, 2000, we located 549 tectonic and 41 low-frequency earthquakes accurately. The magnitude of each event was determined by measuring the maximum amplitude of P or S wave (Watanabe, 1971). Hypocenters for low-frequency and tectonic earthquakes are separately shown in Figs. 5 and 6, respectively.

The coverage of stations was varied in time, as shown in Fig. 2, and the seismicity in the studied period was so active that there was usually large ambient noise. Errors in event locations on March 31 (i.e., with the poorest coverage of stations) in N–S, E–W and depth directions are estimated to be as large as 100, 50 and 300 m, respectively, as standard errors in the least-square determination of locations. Errors for events after April 1 are improved to be about 40, 30 and 150 m, respectively. The errors for low-frequency and tectonic earthquakes are shown in Figs. 7 and 8, respectively. Standard errors are systematically large for events shallower than 2 km. Since the average interval of our stations is about 2 km (Fig. 1), all the rays used in the location determination of such shallow events take off downwards and their errors, particularly in depth, become very large. The onset of low-frequency earthquakes is generally obscure, compared to that of tectonic ones, so their location errors (Fig. 7) are about 1.25–2 times those of tectonic ones (Fig. 8). RMS values for tectonic events before and after April 1 are about 0.1 s and less than 0.05 s, respectively. This improvement of hypocentral determination is mainly

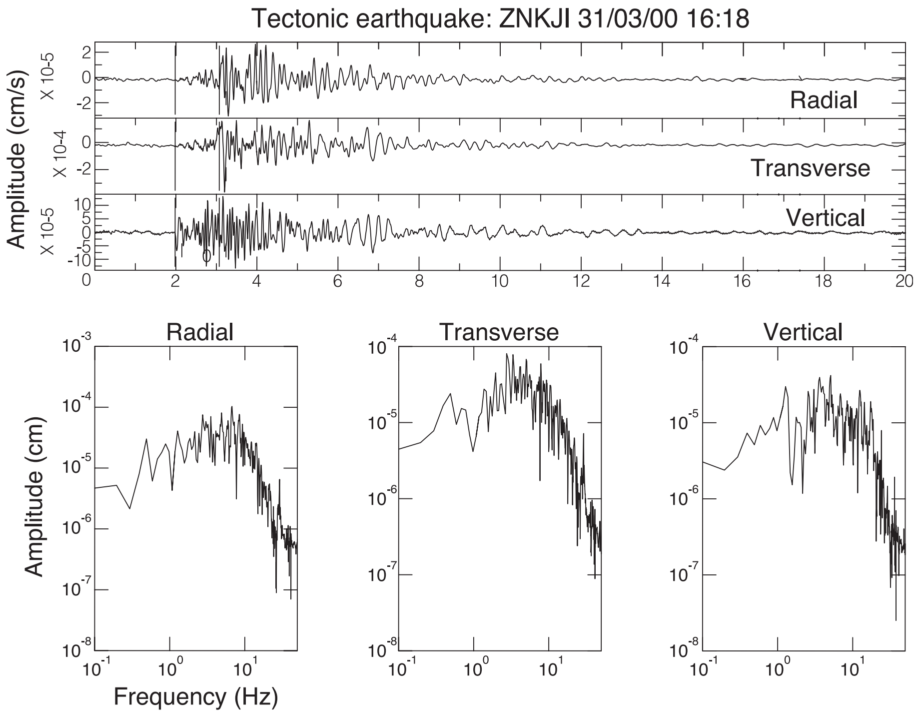

Fig. 4. Same as Fig. 3 except for a tectonic earthquake.

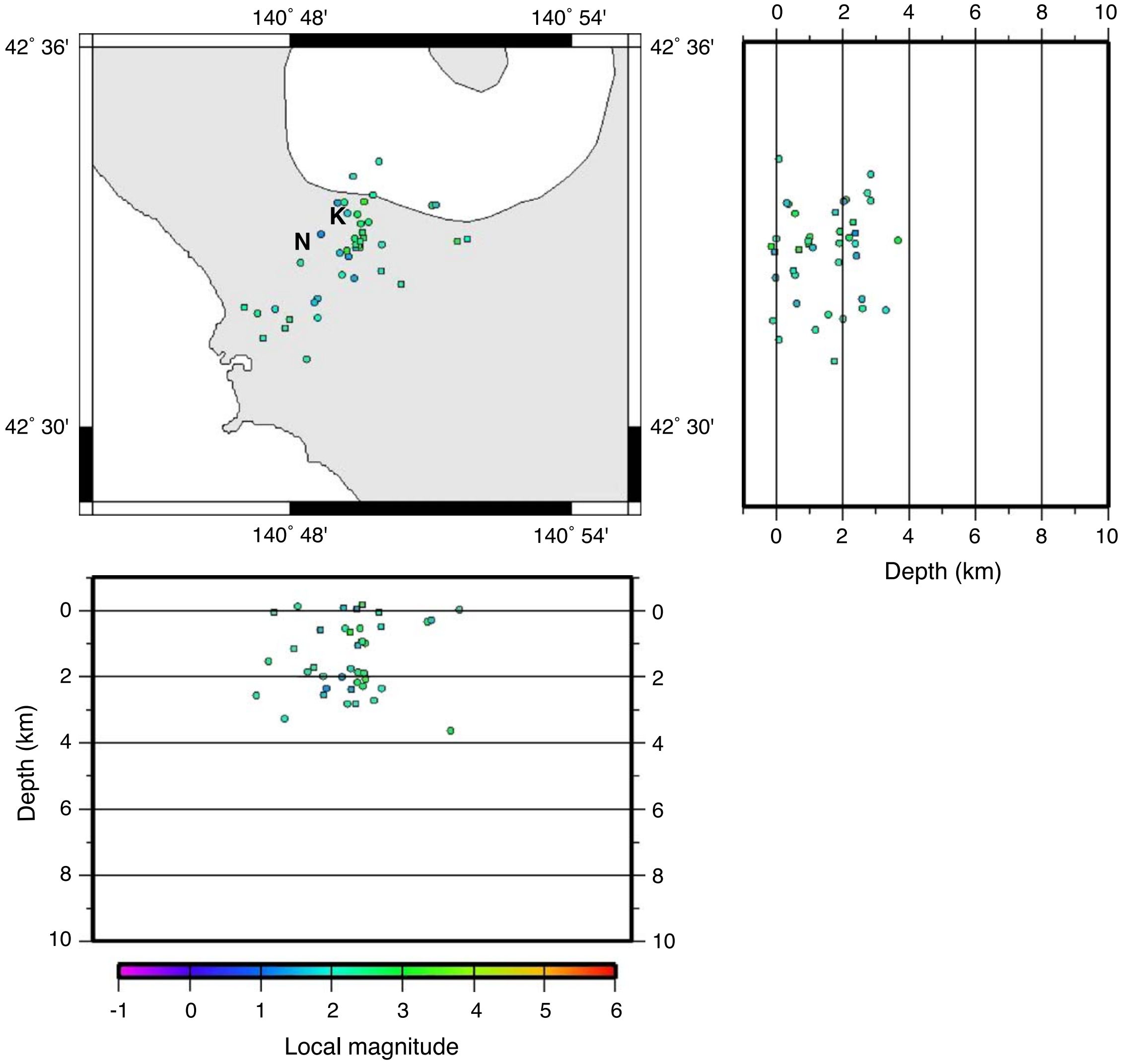

Fig. 5. Hypocenter locations of 41 low-frequency earthquakes determined in this study with local magnitude in color.

due to the additional installation of seismometers and to the reduced background noise.

Comparing Fig. 5 with Fig. 6, locations of low-frequency earthquakes are clearly different from those of tectonic ones, as also pointed out by Oshima (2000) with the ISV local network. In the 2000 eruption of Mt. Usu, new craters were created in the northwestern mountain flank, which are indicated by characters of "N" and "K" in Fig. 1 with the timings shown in Fig. 2. They started being formed just after the first surface eruption on March 31. Low-frequency earthquakes are mostly located just in the southeast of these craters, confined in a nearly vertical and narrow zone of about 500 m wide and 4 km long with the trend of NNE–SSW (Fig. 5). All of them are shallower than 4 km. Using different data sets from ours, both Yoshida et al. (2002) and Oshima (2000) obtained the similar spatial distributions for low-frequency earthquakes.

In contrast, tectonic earthquakes are distributed in a much larger area, particularly extending in the southeast of the craters. There appears to exist a zone of no seismicity just in the south of the craters, resulting in a

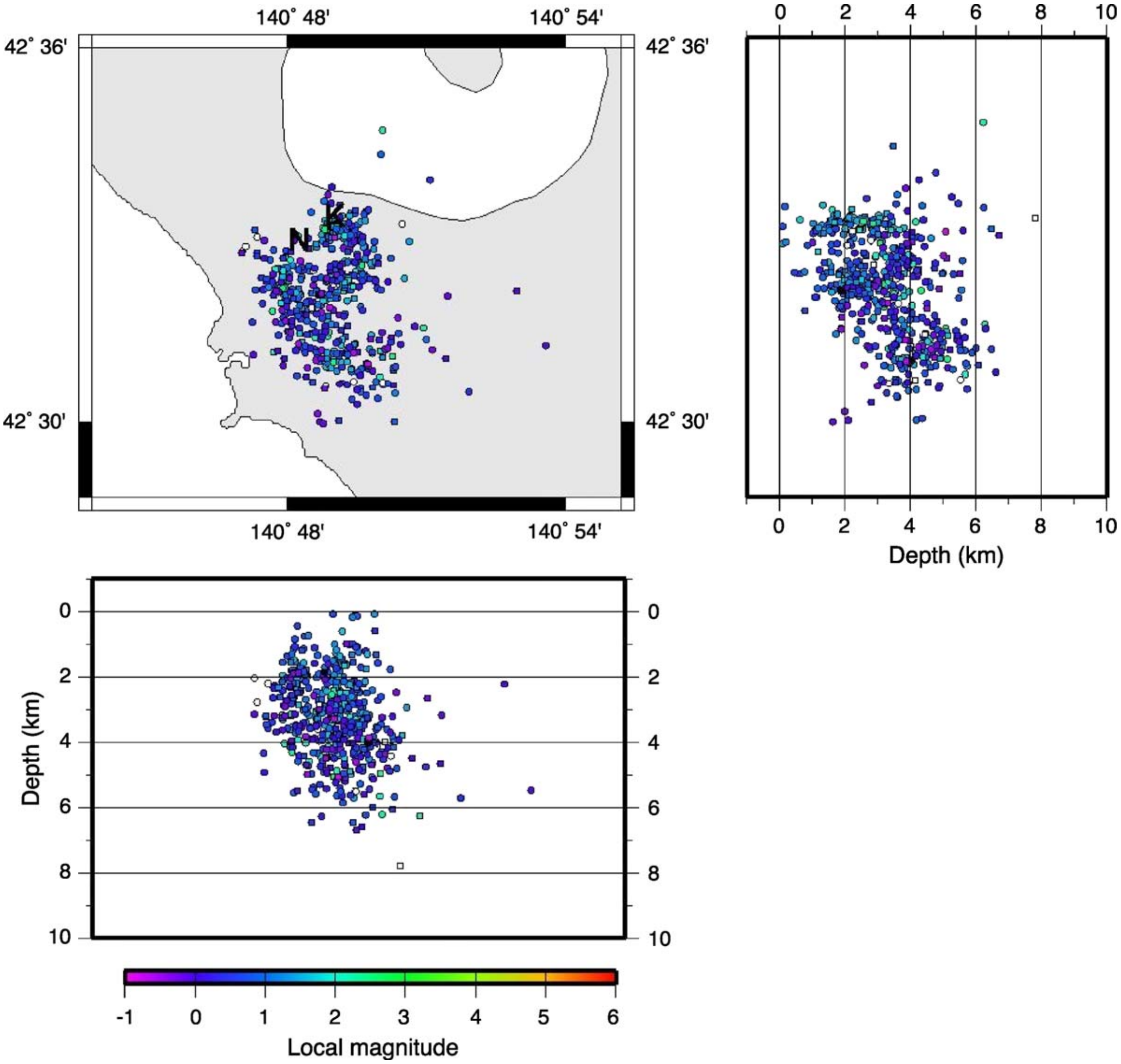

Fig. 6. Same as Fig. 5 except for 549 tectonic earthquakes.

donut-like shape. Some low-frequency earthquakes occurred in the area where tectonic ones were missing. The distribution of tectonic earthquakes tends to become deeper in the south of the craters, and some of them are as deep as 8 km.

Small tectonic earthquakes began to occur in the south of Mt. Usu on April 2. Since they occurred in an area far from the craters and were distributed in a widespread area, they are likely not to be directly related to magma activities but to be originated from the regional tectonic stress field affected by the intrusion of a magma body near the craters. While normal earthquakes were still active after April 5, we could hardly find any low-frequency ones after April 2 in the present data set. This implies that most of the magma activities responsible for the 2000 Mt.Usu eruption should have terminated around April 2. GPS observation of crustal deformation (Okazaki et al., 2002) and gravity measurement (Koyama et al., 2002) also support such a

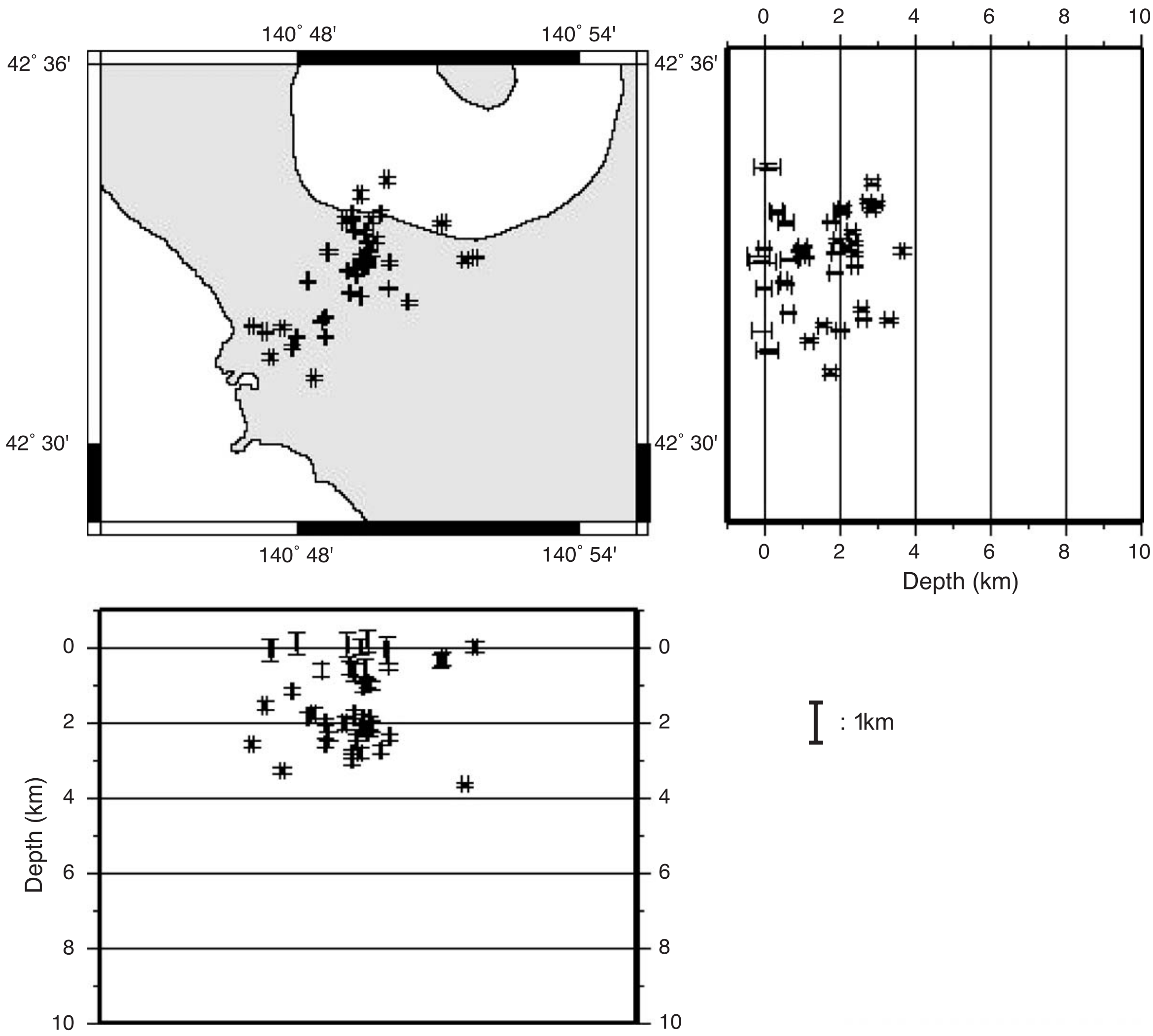

Fig. 7. Same as Fig. 5 except for each location with standard errors.

termination timing of magma activities. On the other hand, low-frequency earthquakes with large recorded amplitude were observed only for several days before (Yoshida et al., 2002) and after the first eruption.

4. Waveform and spectrum with site correction

In this chapter, we discuss major characteristics in waveform and spectrum of low-frequency and tectonic earthquakes. Figs. 9 and 10 show running spectrograms of the vertical seismogram for the low-frequency earthquake of Fig. 3 and a record of the same record length with at least one tectonic earthquake, respectively. As for these examples, durations of low-frequency earthquakes (~ 40 s) are generally nearly twice those of the tectonic (~ 15 s) with the same local magnitude. While the predominant frequency of low-frequency earthquakes is 1.0–2.5 Hz, there are no sharp predominant spectral peaks for tectonic earthquakes. Substantial amounts of spectra are observed for tectonic ones at frequency higher than 5 Hz, as shown in Fig. 10.

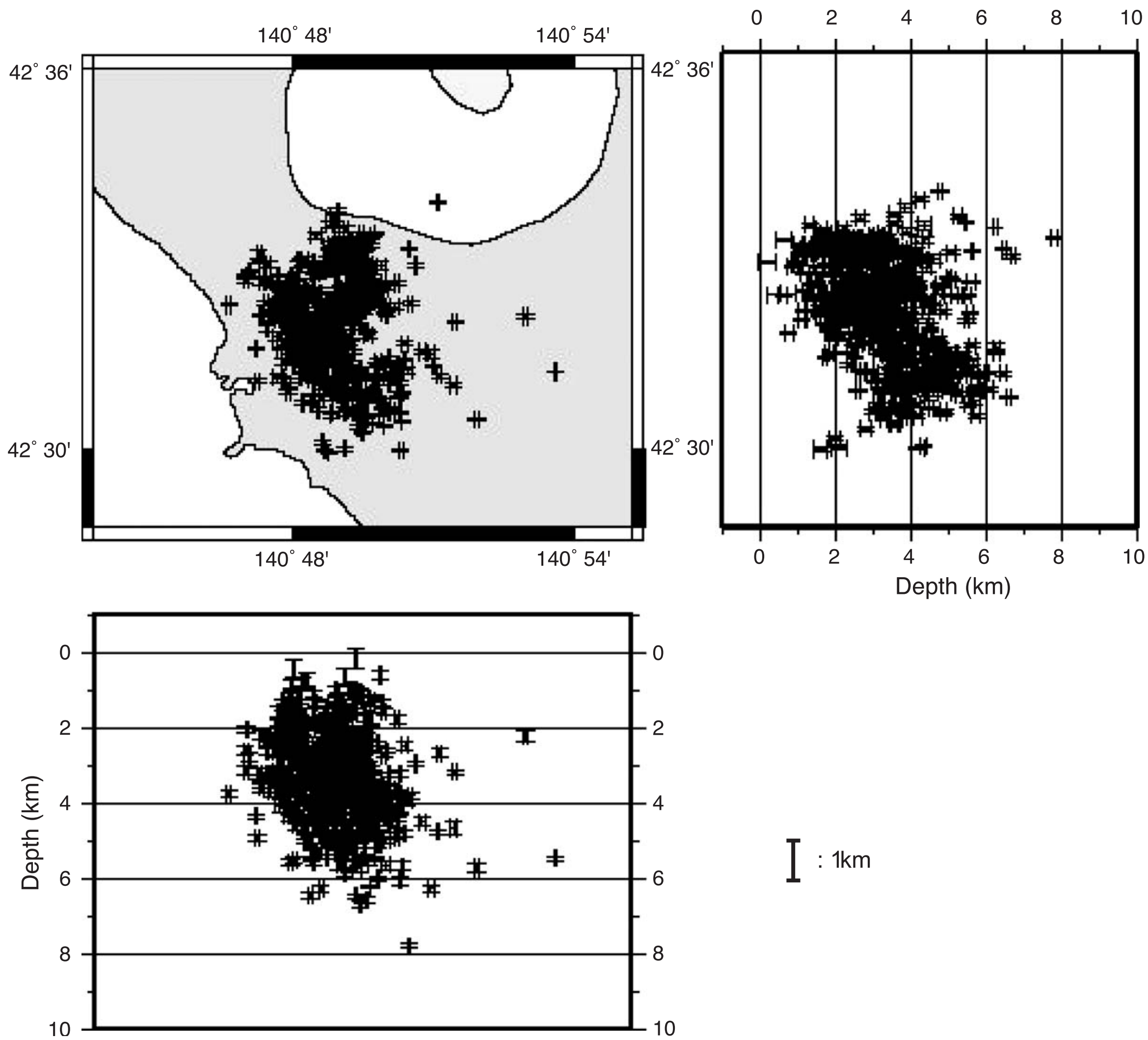

Fig. 8. Same as Fig. 6 except for each location with standard errors.

Since original seismograms are affected by not only source process but also complex propagation effect from a source region to each station, as well as near-surface complex structure beneath each station, so-called site effect. The site effect is particularly strong for stations in a volcanic area. In order to estimate the source process of these events better, we attempt to remove the first-order site effect of each station from original seismograms with the use of records for a teleseismic event.

The amplitude spectrum, $A_j\,(f)$, observed at the jth station for a given seismic event can be generally written as (Bath, 1974):

$$A_j(f) = G_j K_j(f) S_j(f) I_j(f) \exp(-\pi f t_j^*) \quad (1)$$

where G_j is the geometrical spreading term, $K_j\,(f)$ is the source spectrum including the radiation pattern to the jth station, $S_j\,(f)$ is the site response, $I_j\,(f)$ is the instrumental transfer function, and $\exp(-\pi f t_j^*)$ is the term taking into account scatter-

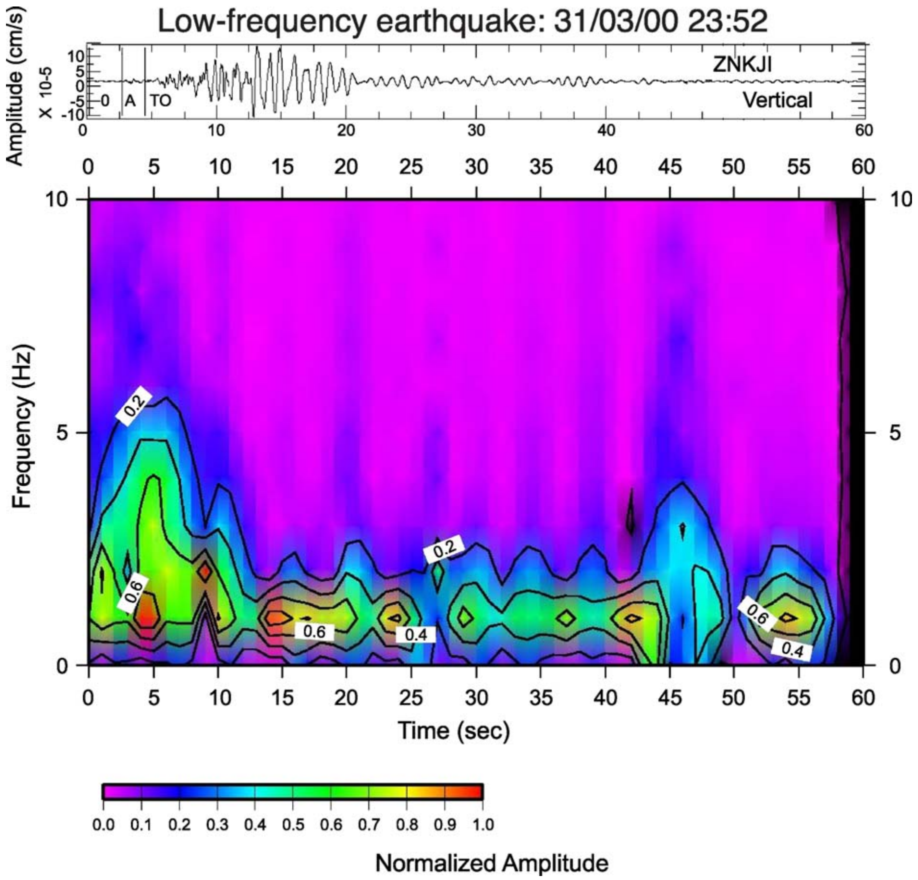

Fig. 9. Running vertical-component spectrograms for the low-frequency earthquake of Fig. 3.

ing loss as well as intrinsic attenuation along the path from the source to the jth station C_j : $t_j^* = \int_{C_j} \frac{\pi ds}{Qv}$, where Q is the quality factor in the path and v is the wave velocity. Since our seismograms were recorded by different systems, we denote that the site response $S_j\ (f)$ includes the instrumental transfer function $I_j\ (f)$.

For an earthquake occurring far from stations (i.e., a teleseismic event), we can approximate that all the three terms, the attenuation term $\exp(-\pi f t_j^*)$, the geometrical spreading term G_j, and the source term with its radiation pattern $S_j\ (f)$ are common among stations, and we take off the subscript j from these quantities. Although we do not obtain any absolute values of site amplification factor $S_j\ (f)$, the *relative* site amplification factor $\mathrm{SAF}_j\ (f)$ at the jth station, with respect to the average site effect over all the stations $\tilde{S}(f)$, can be obtained from the following spectral ratio:

$$\frac{A_j(f)}{\tilde{A}(f)} = \frac{GK(f)S_j(f)\exp(-\pi f t^*)}{\frac{1}{N}\sum_{j=1}^{N} GK(f)S_j(f)\exp(-\pi f t^*)} = \frac{S_j(f)}{\frac{1}{N}\sum_{j=1}^{N} S_j(f)} = \frac{S_j(f)}{\tilde{S}(f)} \equiv \mathrm{SAF}_j(f) \qquad (2)$$

where $\tilde{A}(f)$ is the amplitude spectrum averaged over all the stations $A_j\ (f)$ for the teleseismic event.

We used a teleseismic event ($M_w = 5.4$) on April 13, 2000, located at 40.1°N, 142.4°E and 50 km deep (Fig. 11), in order to estimate the relative site

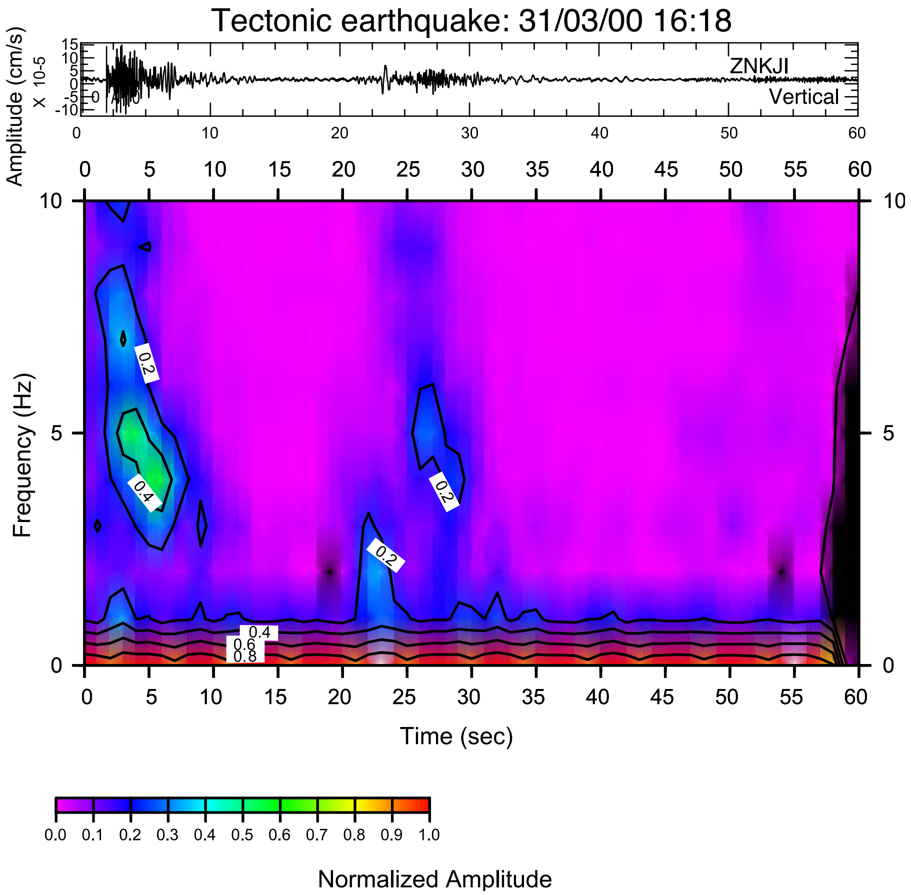

Fig. 10. Same as Fig. 9 except for a record with at least one tectonic earthquake.

amplification factor of each station. Clear seismograms were recorded for this event at all the five broadband stations (ABUTA, HANAW, KORYO, SHNZN, ZNKJI), four JMA stations (HGSN, JMAA, UJE1, UJE2) and one ISV station (HNWD). Fig. 11 shows an example, recorded at ZNKJI, of these seismograms. We take the time window of 10 s from the onset of S wave in the calculation of amplitude spectra $A_j(f)$. Since the raw spectrum of each seismogram generally has many peaks and troughs particularly at high frequency, as shown in Fig. 11, we smoothed spectra $A_j(f)$ by averaging over five adjacent points for each spectral point. Taking the average of these spectra over all the observed stations for the denominator of Eq. (2), the site amplification factor $SAF_j(f)$ is estimated for the jth station.

The site amplification factor $SAF_j(f)$ estimated for a broadband seismic station (ZNKJI) is shown in Fig. 12, together with the site-corrected S-wave spectra for the low-frequency earthquake of Fig. 3. There are no remarkable spatial patterns of $SAF_j(f)$, in spite of large variations by a factor of more than 10, particularly in a frequency range lower than 1 Hz, partly because $SAF_j(f)$ in our definition includes the instrumental transfer function in $S_j(f)$. High-frequency components at ZNKJI are amplified, particularly in horizontal components, compared with the original spectra of Fig. 3, due to small values of its site amplification factors. The frequencies of major spectral peaks (0.5–2 Hz in this example) appear to be invariant by the present site correction while relative amplitudes and widths of these spectral peaks are much changed in some cases. Such spectral character-

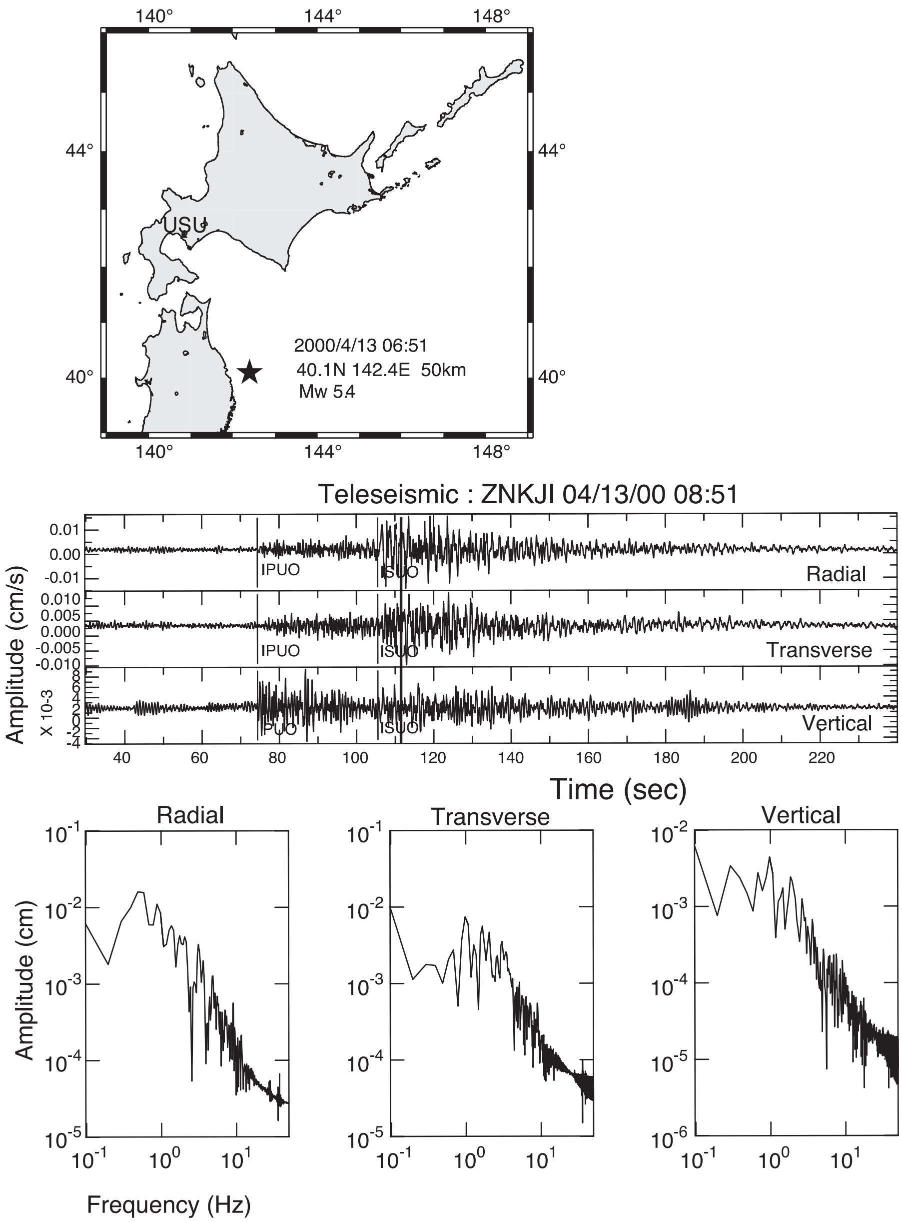

Fig. 11. Location of the teleseismic event at 6:51 on April 13, 2000, for the estimation of the site amplification factor at each station, and its waveforms and S-wave spectra at ZNKJI.

istics are critical in the quantitative estimation of some parameters to describe the source process of low-frequency earthquakes (e.g., crack length and fluid viscous damping loss, see details in Chouet et al., 1994; Matsubara and Yomogida, 2004), implying the importance of the site correction.

Complex path effects, which we do not consider here, may alter the overall feature of observed spectra very much, but they are unlikely to be highly frequency-dependent and affect major observed spectral peaks. Although we cannot deny the other possibilities, the spectral peaks after the above site correction

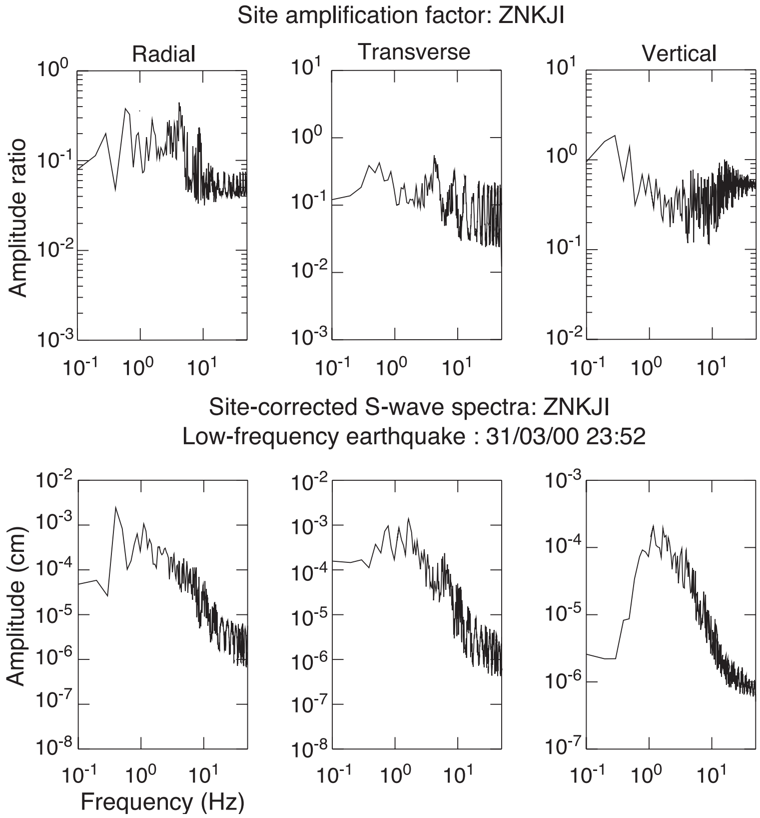

Fig. 12. Estimated three-component site amplification factor at ZNKJI, and the site-corrected S-wave spectra for the low-frequency event of Fig. 3.

(e.g., Fig. 12) should reflect major features of the source process of low-frequency earthquakes.

5. Magma activities and deep crustal earthquakes

The difference in both hypocentral location and their waveform/spectrum between low-frequency and tectonic earthquakes suggests that their source process should be very different. While tectonic ones are caused by the change of ambient tectonic stress due to mass movement of magma, low-frequency earthquakes may be directly related to magma activities because no such events are found in non-volcanic areas. As shown in Fig. 5, low-frequency earthquakes occurred only in a nearly vertical, narrow and shallow (<4 km) zone with a NNE–SSW trend, suggesting that their locations may directly correspond to either magma or hydrothermal activities underneath Mt. Usu. The magma associated in the 2000 eruption seems to have formed a plane- or sheet-like structure, at least during the present observation period (i.e., for 6 days just after the first surface eruption).

Most of tectonic earthquakes, especially those after April 2, probably occurred where pre-stress or ambient tectonic stress had been large, and they were triggered by the stress change due to the upward migration of magma. In the further south of the summit of Mt. Usu, the seismicity of tectonic earthquakes continued for a while, including the largest event on April 1 during the 2000 eruption even after low-frequency earthquakes no longer occurred. In this area, tectonic earthquakes may have been caused by the reactivation of pre-existing faults.

If low-frequency earthquakes are somehow related to magma activities of the 2000 Mt. Usu eruption, their waveforms or spectra provide quantitative information of their source process. Waveforms of low-frequency earthquakes show an early part of high-frequency waves followed by low-frequency waves of long duration (Fig. 13). While the high-frequency waves are generally characterized by the predominant frequency of about 4–5 Hz and duration less then 5 s, the predominant frequency is about 1 Hz and its duration longer than 20 s for the low-frequency. These characteristics are clearly seen at stations located in the west (e.g., MTYD, Fig. 13a, HNWD) and south-east (e.g., KORYO, SHNZN, Fig. 13b) of their hypocenters, but the early high-frequency waves are not clear or weak at stations in the south (e.g., ZNKJI, Fig. 13c), regardless of their epicentral distances. Tectonic earthquakes of hypocentral locations similar to low-frequency earthquakes do not show this type of directivities, implying that the above azimuthal variation of low-frequency earthquakes is not due to path effects, but their source process should be responsible. This is the strong evidence of non-isotropic source radiation, and it is consistent with the plane-like magma distribution estimated from their event locations (Fig. 5).

The above characteristics were also observed for low-frequency earthquakes, called hybrid earthquakes and LP earthquakes, at Mt. Redoubt in Alaska (Chouet, 1996). The predominant frequencies of early high-frequency and later low-frequency parts were about 6–8 Hz and about 1 Hz, respectively, for the hybrid earthquakes. Their directional variations are also quite similar to those at Mt. Usu. Chouet (1988) discussed that they were caused by the resonance of a crack filled with fluid of Chouet (1986), and the low-frequency earthquakes at Mt. Usu can be also explained well by the same model (Matsubara and Yomogida, 2004).

Turning our attention to long-term activities of Mt. Usu from seismological points of view, we found some precedent deep crustal seismic activities beneath it. Anomalous deep events beneath active volcanoes in Japan have been detected in the lower crust where earthquake activities were believed not to exit (hereafter called ‘‘deep crustal low-frequency earthquakes’’). Their dominant frequency (>2.5 Hz) is lower than shallow tectonic earthquakes, and there are no clear P- or S-wave onsets (e.g., Ukawa and Ohtake, 1987; Hasegawa and Yamamoto, 1994). Previous studies suggested that such deep events are related to magma movements because they have been detected only beneath recently active volcanoes.

Such deep events occurring in and around Hokkaido, Japan, have been routinely reported since October 1997 by Sapporo District of Meteorological

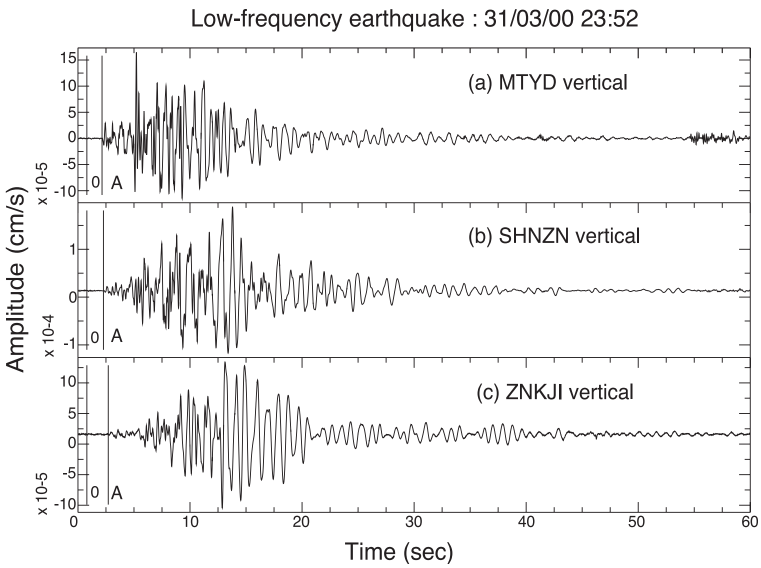

Fig. 13. Vertical-component waveforms for the low-frequency earthquake of Fig. 3 at three stations. Comparing the waveforms during 5 s from the P-wave onset, high-frequency part exists in (a) MTYD and (b) SHNZN but not clear in (c) ZNKJI.

Observatory, including their hypocentral depths and predominant frequency. Takahashi et al. (1999) carefully re-examined those listed deep crustal low-frequency earthquakes up to August 1999, using the combined seismic waveform data of Sapporo District of Meteorological Observatory and ISV (Hokkaido University), Tohoku University and Hirosaki University. They identified 25 deep crustal low-frequency earthquakes during the period from October 1, 1997 to June 20, 1998.

These earthquakes in the Hokkaido area have the following major characteristics: (1) the predominant frequency of about 1.0–2.5 Hz, (2) focal depth range of about 20–40 km, (3) local magnitude less than 2.5, (4) non-episodic occurrence, for example, two or more events at a small area within a short time interval and (5) located beneath Quaternary active volcanoes. Takahashi et al. (1999) also pointed out that several deep crustal low-frequency earthquakes occurred 1 or 2 years before surface volcanic activities above them.

Materials in a depth range of 20–40 km must be ductile, and tectonic earthquakes in terms of brittle failure are unlikely to occur there (Shimamoto, 1986). From their fault mechanisms, these low-frequency events are considered not due to tectonic shear faulting, but magma activities are at least partly involved (e.g., Suzuki, 1992; Sato and Hasegawa, 1996).

We checked seismic waveform data collected by Sapporo District of Meteorological Observatory and ISV, Tohoku University and Hirosaki University, in

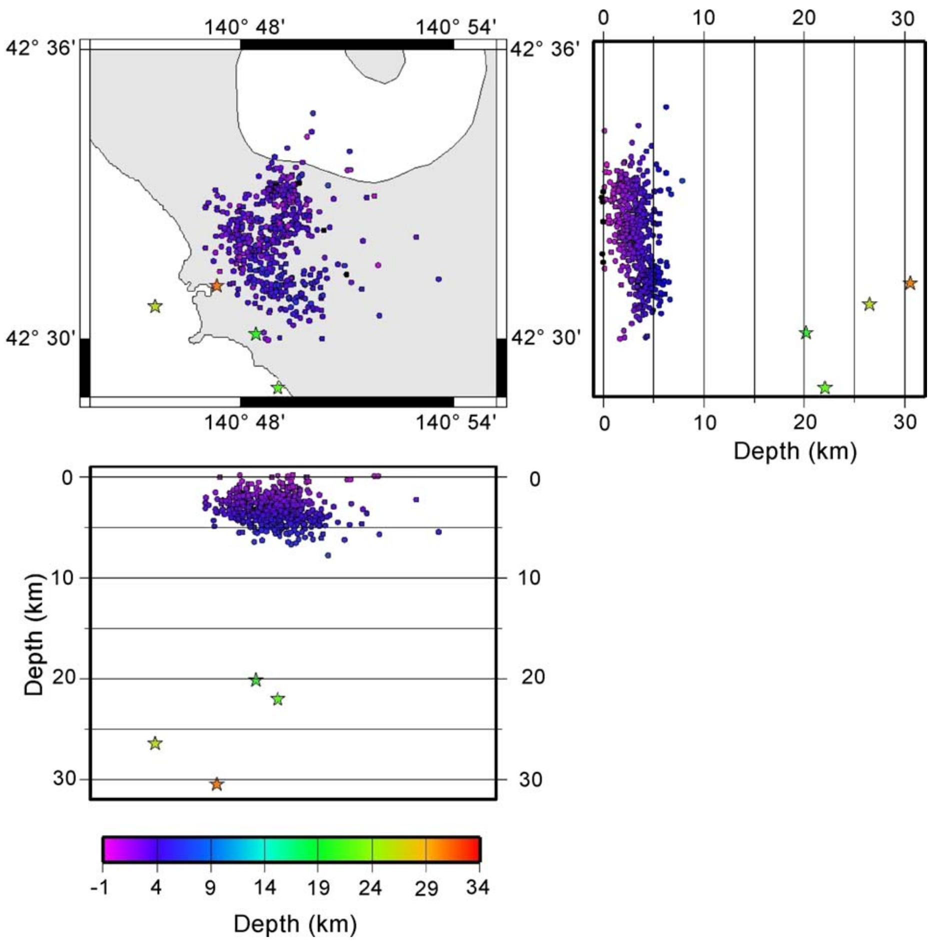

Fig. 14. Distribution of all earthquakes associated with the 2000 eruption of Mt. Usu (circles), together with four deep crustal low-frequency earthquakes beneath Mt. Usu (stars).

order to carefully investigate the characteristics of deep crustal events in and around Mt. Usu from October 20, 1997 to August 16, 1999. During this period, 125 deep crustal low-frequency earthquakes in and around Hokkaido were listed by the routine data processing of Sapporo District of Meteorological Observatory, including four events located near Mt. Usu. These four earthquakes occurred within 3 min on October 17, 1998. Their local magnitudes are 1.4–2.2, and their focal depths are 20–30 km. We picked P-wave onset times and relocated their locations, as shown in Fig. 14. There were only a few stations in operation around the hypocentral area then, unlike the eruption period, and all the onsets are very obscure, as shown in Fig. 15. For these reasons, the uncertainty in hypocentral location is 2–3 km in horizontal directions and as large as 5 km in depth. It may be possible that the locations of the four events are much closer to each other than Fig. 14.

We could analyze waveforms of only two of the four events with relatively clear P-wave onsets and much larger amplitude than ambient noise. Predominant frequencies of the two events are estimated to be 1.0–2.0 Hz in the S-wave spectra (Fig. 15). We confirmed that these waveforms and spectral characteristics are similar to deep events that occurred near Mt. Komagatake, one of the most active volcanoes in Hokkaido, Japan. These values are also similar to the events reported in Izu-Ooshima (Ukawa and Obara, 1993) and in Mt. Iwate (Hasegawa et al., 1991) before their eruptions. Although we cannot deny the existence of other small deep crustal events beneath Mt. Usu, the four events on October 17, 1998 shown in Fig. 14 were at least the largest for the past 4 years before the 2000 eruption.

Both GPS observations and geological studies implied that there are two major magma chambers beneath Mt. Usu, located 4 and 12 km deep (e.g., Tomiya and Miyagi, 2002), respectively. For example, the GPS observation of Okazaki et al. (2002) suggested that the shallow magma chamber (4 km deep) was responsible for the first eruption in 2000, followed by the magma supply from the deep one. By a continuous GPS observation from 1982 to 1999, the summit of Mt. Usu took downward motions or subsidence with the rate up to 8 cm/year (Mori and Ui, 2000). These long-term observations at the surface supported the idea that the 2000 eruption of Mt. Usu was triggered by the subsidence of the volcanic body itself.

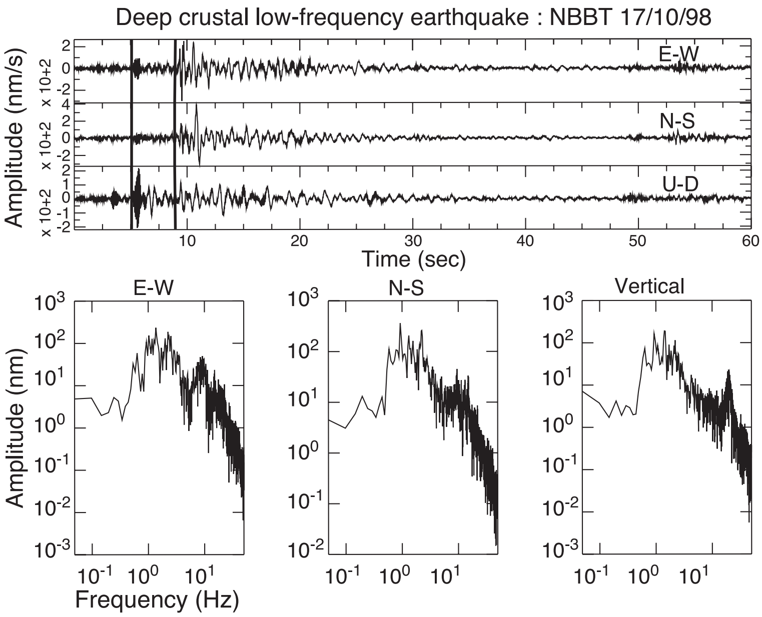

Fig. 15. Seismograms and S-wave spectra of a deep crustal low-frequency earthquake at 1:51 on October 17, 1998, recorded at a JMA short-period seismic station, NBBT.

Although the 2000 eruption may not be directly related to the upward magma migration from the lower crust, we cannot deny the role of some magma supply to the 12 km deep magma chamber implied by the four large deep crustal low-frequency earthquakes in this area. In this case, the upward migration of the magma from the depth of about 30 km seems to have been so episodic and local that any related surface deformations were not detected by GPS observations during this period. As a similar previous example, Ukawa and Ohtake (1987) related deep crustal low-frequency earthquakes of about 32 km in depth located beneath Izu-Ooshima volcano on August 1987 to its eruption about 1 year later. Although the relation between deep crustal events and surface eruption may be still speculative, it is still a worthwhile avenue of enquiry, particularly because recent high-density and sensitive seismic networks are revealing the nature of very weak deep crustal events (e.g., Obara, 2002).

6. Conclusions

We located 590 events, including 41 low-frequency earthquakes, associated with the 2000 eruption of Mt. Usu. Low-frequency and tectonic earthquakes are quite different in both location and waveform. Low-frequency earthquakes were distributed in a nearly vertical narrow zone near the craters while tectonic ones in a much larger area around the craters in a donut-like form. Hypocenters of low-frequency earthquakes were shallower than 4 km. Tectonic ones occurred as deep as 8 km, getting deeper in south. The locations of low-frequency earthquakes grossly correspond to the area of no seismicity of tectonic ones, that is, the center of the donut. Temporal patterns of the two types were also very different: tectonic earthquakes continued for about 1 month after the first eruption, but low-frequency earthquakes diminished within 2 or 3 days.

S-wave spectra of low-frequency earthquakes have one or two clear predominant frequencies of 0.5–2 Hz while tectonic ones do not have any clear spectral peaks with much energy of frequency higher than several Hz. From characteristics in waveform and spectrum, the source process of low-frequency earthquakes associated with the 2000 eruption of Mt. Usu seems to be similar to that of hybrid and LP events at Mt. Redoubt in Alaska, which were considered to be caused by the resonance of fluid-filled cracks (Chouet, 1986). Their spatial distribution at Mt. Usu (i.e., a nearly vertical plane directed in NNE–SSW and shallower than 4 km) indicates the existence of a shallow magma body responsible for the 2000 eruption. Such magma activities terminated in 2 or 3 days after the first eruption, which is consistent with other observations such as gravity measurement (e.g., Koyama et al., 2002).

In addition, we found four deep crustal low-frequency earthquakes that occurred on October 17, 1998 near Mt. Usu with the focal depth of 20–30 km. As proposed for other active volcanoes in Japan, they may be related to the 2000 eruption or future eruptions of Mt. Usu, reflecting at least a part of its deep magma activities.

Acknowledgements

The authors sincerely thank Takeo Moriya for his help with installing broadband seismometers and Kunikazu Yoshida for his helpful comments on the original draft. Comments by Shigeki Horiuch and one anonymous reviewer are greatly appreciated. We were allowed to use Broadband seismometer systems through the kindness of Yuichi Morita. We used the data of JMA (Japan Meteorological Agency) recorded in and around Mt. Usu. This study was partly supported by the Institute of Seismology and Volcanology, Hokkaido University.

References

Aki, K., Koyanagi, R., 1981. Deep volcanic tremor and magma ascent mechanism under Kilauea, Hawaii. J. Geophys. Res. 86, 7095–7109.

Bath, M., 1974. Spectral Analysis in Geophysics. Elsevier, Amsterdam.

Chouet, B., 1986. Dynamics of a fluid-driven crack in three dimensions by the finite difference method. J. Geophys. Res. 91, 13969–13992.

Chouet, B., 1988. Resonance of a fluid-driven crack: radiation properties and implications for the source of long-period events and harmonic tremor. J. Geophys. Res. 93, 4375–4400.

Chouet, B., 1996. Long-period volcano seismicity: its source and use in eruption forecasting. Nature 380, 309–316.

Chouet, B., Stephens, C.D., Lahr, J.C., Power, J.A., 1994. Precursory swarms of long-period events at Redoubt Volcano (1989–1990), Alaska: their origin and use as a forecasting tool. J. Volcanol. Geotherm. Res. 62, 95–135.

Geological Survey of Hokkaido, 2000. The eruption of Mt. Usu. Newsletter, Geological Survey of Hokkaido. Special Issue, vol. 16, pp. 1–9.

Goldstein, P., Dodge, D., Firpo, M., 1999. SAC2000: Signal processing and analysis tools for seismologists and engineers. International Handbook of Earthquake and Engineering Seismology. UCRL-JC-135963, Invited contribution to the IASPEI.

Hasegawa, A., Yamamoto, A., 1994. Deep, low-frequency microearthquakes in or around seismic low-velocity zones beneath active volcanoes in northeastern Japan. Tectonophysics 233, 233–252.

Hasegawa, A., Zhao, D., Yamamoto, A., Horiuchi, S., 1991. Deep structure of volcanoes and its relation to the occurrence of crustal earthquakes in the northeastern Japan arc as inferred from seismic observations. Kazan 36, 197–210.

Hirata, N., Matsu'ura, M., 1987. Maximum-likelihood estimation of hypocenter with origin time eliminated using nonlinear inversion technique. Phys. Earth Planet. Inter. 47, 50–61.

Kaneshima, S., Kawakatsu, H., Matsubayashi, H., Sudo, Y., Tutui, T., Ohminato, T., Ito, H., Uhira, K., Yamasato, H., Oikawa, J., Takeo, M., Iidaka, T., 1996. Mechanism of phreatic eruptions at Aso Volcano inferred from near-field broadband seismic observations. Science 273, 642–645.

Kawakatsu, H., Ohminato, T., Ito, H., Kuwahara, Y., Kato, T., Tsuruga, K., Honda, S., Yomogida, K., 1992. Broadband seismic observation at the Sakurajima volcano, Japan. Geophys. Res. Lett. 19, 1959–1962.

Kawakatsu, H., Kaneshima, S., Matsubayashi, H., Ohminato, T., Sudo, Y., Tutui, T., Uhira, K., Yamasato, H., Ito, H., Legrand, D., 2000. Aso-94: Aso seismic observation with broadband instruments. J. Volcanol. Geotherm. Res. 101, 129–154.

Koyama, J., Yomogida, K., Moriya, T., Takada, M., Ichiyanagi, M., Furuya, M., 2002. Time constant of the 2000 eruption activity of Volcano Usu (in Japanese, with English Abstr.). Kazan 47, 587–594.

Matsubara, W., Yomogida, K., 2004. Source process of low-frequency earthquakes associated with the 2000 eruption of Mt. Usu. J. Volcanol. Geotherm. Res. 134, 223–240.

Mori, Y.H., Ui, T., 2000. Crustal deformation and eruptic activities of Mt. Usu in 2000 (in Japanese with English Abstr.). J. JSNDS 19-3, 383–390.

Obara, K., 2002. Nonvolcanic deep tremor associated with subduction in southwest Japan. Science 296, 1679–1681.

Ohminato, T., Chouet, B., Dawson, P., Kedar, S., 1998. Waveform inversion of very long period impulsive signals associated with magmatic injection beneath Kilauea Volcano, Hawaii. J. Geophys. Res. 103, 23839–23861.

Okada, H., Watanabe, H., Yamashita, H., Yokoyama, I., 1981. Seismological significance of the 1977–1978 eruptions and the magma intrusion process of Usu Volcano, Hokkaido. J. Volcanol. Geotherm. Res. 9, 311–334.

Okazaki, N., Takahashi, H., Kasahara, M., Ishimaru, S., Mori, H.Y., Kitagawa, S., Fujiwara, K., Churei, M., 2002. Crustal deformation associated with the 2000 eruption of Usu Volcano as observed by a dense GPS array (in Japanese, with English Abstr.). Kazan 47, 547–557.

Oshima, H., 2000. Seismic activity associated with the 2000 eruption of Mt. Usu (in Japanese). Newsletter, Seismol. Soc. Jpn. 12, 23–24.

Sato, H., Hasegawa, A., 1996. Mapping of partial melt zones in the upper mantle beneath northeastern Japan ascent of magma in island arc (in Japanese, with English Abstr.). Kazan 41, 115–125.

Shimamoto, T., 1986. Transition between frictional slip and ductile flow forhalite shear zones at room temperature. Science 231, 711–714.

Suzuki, S., 1992. Low-frequency microearthquakes occurring near the Moho boundary beneath Tokachi-dake volcano, Hokkaido (in Japanese, with English Abstr.). Kazan 37, 9–20.

Takahashi, H., Miyamura, J., Gouke, K., 1999. Deep low frequency microearthquakes occurring in Hokkaido (in Japanese, with English Abstr.). Geophys. Bull. Hokkaido Univ., Jpn. 62, 25–41.

Tomiya, A., Miyagi, I., 2002. The eruptive products and magma process of March 31, 2000 eruption of Usu Volcano (in Japanese, with English Abstr.). Kazan 47, 663–673.

Tsuruga, K., Yomogida, K., Honda, S., Ito, H., Ohminato, T., Kawakatsu, H., 1997. Spatial and temporal variations of volcanic earthquakes at Sakurajima volcano, Japan. J. Volcanol. Geotherm. Res. 75, 337–358.

Ukawa, M., Obara, K., 1993. Low frequency earthquakes around Moho beneath the volcanic front in the Kanto district, central Japan (in Japanese, with English Abstr.). Kazan 38, 187–197.

Ukawa, M., Ohtake, M., 1987. Monochromatic earthquake beneath Izu-Ooshima. J. Geophys. Res. 92, 12349–12663.

Urabe, T., Tsukada, S., 1991. A workstation-assisted processing system for waveform data from microearthquake networks (in Japanese). Abstr. Seis. Soc. Jpn. 1, 70.

Watanabe, K., 1971. Determination of earthquake magnitude at regional distance in and near Japan (in Japanese, with English Abstr.). Kazan 24, 189–200.

Yamamoto, M., Kawakatsu, H., Yomogida, K., Koyama, J., 2002. Long-period (12 sec) volcanic tremor observed at Usu 2000 eruption: Seismological detection of a deep magma plumbing system. Geophys. Res. Lett. 29, 43-1–43-4.

Yokoyama, I., Seino, M., 2000. Geophysical comparison of the three eruptions in the 20th century of Usu Volcano, Japan. Earth Planets Space 52, 73–89.

Yoshida, K., Sasatani, T., Ichiyanagi, M., Oshima, H., Tamura, M., 2002. Low frequency earthquakes excited by eruptive activities of Mt. Usu in 2000 (in Japanese, with English Abstr.). Kazan 47, 507–519.